PACS numbers: 75.10.Jm, 75.50.Ee
DOI: 10.1070/PU2002v045n11ABEH001210

Defects in spin-gap magnets: multispin clusters

A I Smirnov, V N Glazkov

1. Introduction

One-dimensional spin chains with Heisenberg antiferromagnetic exchange have a singlet ground state with strong quantum spin fluctuations. No magnetic order exists in this state, and the average value of the projection of the spin at a site is zero. The ground state of a chain of spins $S = 1$ is separated from the excited triplet states by an energy gap (the Haldane gap) [1]. A homogeneous chain of spins 1/2 has a gapless spectrum [2], while the dimerized (alternating) chain has a spin gap [3]. In spin-gap systems, the magnetic correlation length is finite. Spin-gap states are stable with respect to weak interchain exchange or anisotropy, while chains with a gapless spectrum become ordered under weak interchain exchange. Spin chains are realized in crystals containing magnetic ions arranged in such a way that the exchange interaction along the chain is much stronger than that in transverse directions. Dimerization of spin chains may be due to the crystal structure and also may spontaneously arise because of a spin-Peierls transition in crystals containing chains of spins 1/2. Below the spin-Peierls transition temperature, dimerization arises because of a gain in exchange energy [4]. At low temperatures the magnetic susceptibility of spin-gap systems 'freezes out,' and these crystals, which contain magnetic ions in each cell, become practically nonmagnetic.

The introduction of impurities into a magnetically one-dimensional quantum-disordered system leads to local destruction of the singlet spin-gap state near the impurity atoms and restores local antiferromagnetic order near defects. Thus, in the vicinity of a defect there appears a cluster of antiferromagnetically correlated spins of the basic matrix. Inside the cluster there are finite average projections of the magnetic-ion spins, and, in addition, the cluster has a finite total magnetic moment. Far from impurity atoms, at distances exceeding the correlation length, the local moments become smaller and thermal fluctuations destroy antiferromagnetic correlations. Thus, at low impurity concentrations and high temperatures, the spin clusters are isolated from each other by disordered regions of the slightly perturbed spin-gap matrix. At sufficiently low temperatures, long-range antiferromagnetic order sets in because of cluster-wing overlap and weak interchain exchange [5–8]. The assumption that magnetic defects that arise near impurity atoms are multispin by nature is corroborated by, say, the anomalous value of the g factor of the spin clusters that are formed in the spin-Peierls magnet $CuGeO_3$ when a small fraction of magnetic ions Cu^{2+} are replaced by Ni^{2+} ions [9, 10]. The anomalous value of the g factor is explained by the multispin nature of magnetic defects. Impurity-induced antiferromagnetic ordering has been intensively studied for the spin-Peierls compound $CuGeO_3$ (e.g., see Refs [11, 12]) and has recently been discovered in the diamagnetically diluted Haldane magnet $PbNi_2V_2O_8$ [13]. In this report we discuss the results of experimental investigations of spin clusters that form when diamagnetic ions are substituted for magnetic ions in the Haldane magnet $PbNi_2V_2O_8$ and of phase separation because of impurity-induced antiferromagnetic ordering in spin-Peierls and Haldane magnets.

2. Spin clusters in the diamagnetically diluted Haldane magnet $PbNi_2V_2O_8$

The interest in defects that formed in a Haldane magnet as a result of diamagnetic dilution, which is equivalent to breaks appearing in spin chains, is related not only to the multispin nature of the defects but also to the hypothesis that the effective spin of the cluster is $S = 1/2$ [14]. This hypothesis has been illustrated by computer simulations done by Miyashita and Yamamoto [15], who showed that in a fragment of a chain of spins $S = 1$, finite average values of the spin projections take place near the ends of the fragment, the values of the spin projections near the break are practically independent of the state of the second end of the fragment of a long chain, and the sum of projections of the spins near one of the fragment's ends is 1/2. Long sections of spin chains have two exponentially close energy levels, one of which is a singlet and the other a triplet. Thus, both in the degeneracy multiplicity and in the possible values of the total spin's projection, the long section of a chain of spins 1 is equivalent to two degrees of freedom with spin $S = 1/2$. The concept of the effective spin 1/2 at the ends of broken Haldane chains is being vigorously discussed to this day (e.g., see Katsumata's review [16]).

By studying paramagnetic resonance spectra, it is possible to determine the effective spin of a magnetic object, since in the presence of crystallographic anisotropy the EPR spectrum proves to be split for the effective spin 1 and unsplit for the effective spin 1/2 (e.g., see Ref. [17]).

Figure 1 displays the magnetic resonance lines for a sample of the Haldane magnet $PbNi_2V_2O_8$ in which some of the magnetic ions Ni^{2+} have been replaced by nonmagnetic ions Mg^{2+}. The data in the figure imply that the introduction of nonmagnetic ions leads to an increase in the magnetic response of the sample — in our case, in the intensity of

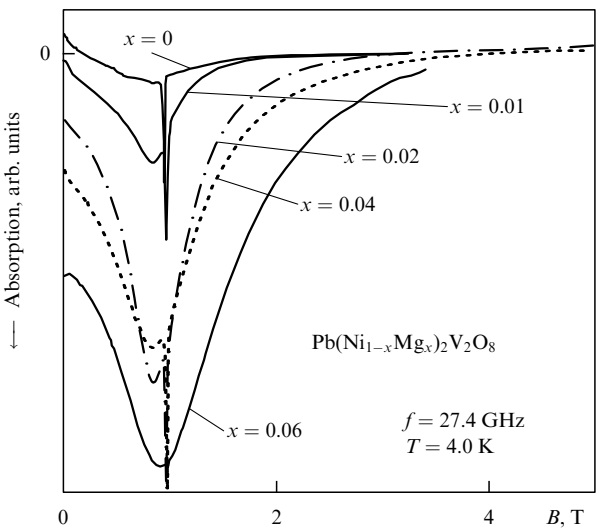

Figure 1. EPR spectra of ceramic samples of $Pb(Ni_{1-x}Mg_x)_2V_2O_8$ with $0 \leqslant x \leqslant 0.06$ at 27.4 GHz and $T = 4$ K. The given value of the temperature exceeds the maximum value of the Néel temperature of 3.5 K for all the investigated samples of $Pb(Ni_{1-x}Mg_x)_2V_2O_8$ (see Ref. [20]). The narrow resonance lines are diphenylpicrylhydrazyl (DPPH) calibration marks corresponding to $g = 2.0$. The absorption signal is normalized to unit weight.

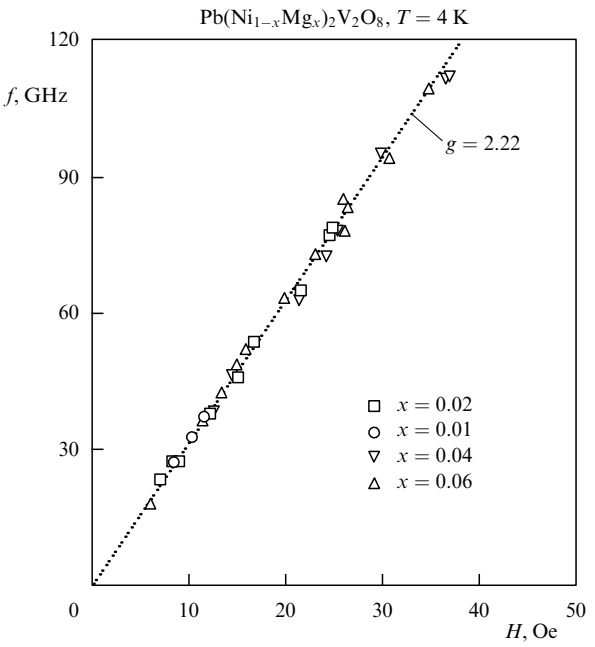

Figure 2. Plot of the resonance frequency vs. the magnetic field strength for ceramic samples of $Pb(Ni_{1-x}Mg_x)_2V_2O_8$ in the paramagnetic phase.

paramagnetic resonance. Measurements of such spectra in the 9 – 110 GHz range make it possible to determine how the paramagnetic-resonance frequency depends on the magnetic field strength. This dependence proved to be the same for all the samples and is shown in Fig. 2: it is linear (with a high accuracy) and passes through the origin. Thus, the data suggest that there is no initial splitting exceeding 0.5 GHz. The initial splitting of the EPR spectrum of an isolated spin $S = 1$ is determined by the term $D(S_z^i)^2$ in the spin Hamiltonian, with D being the single-ion anisotropy constant, which is determined by spin–orbit coupling. The order of magnitude of the initial splitting can be found by using the value $D = -0.23$ meV, which was found by Uchiyama et al. [13] from their measurements of the magnetic excitation spectrum in neutron scattering experiments. The above value of the single-ion anisotropy constant corresponds to an initial splitting of the paramagnetic resonance of spin $S = 1$ of about 50 GHz. With such initial splitting, one should observe an extremely broad absorption line for a ceramic sample, a result incompatible with the resonance lines in Fig. 1. Thus, the resonance lines without initial splitting shown in Fig. 1 suggest that the effective spin arising at the ends of broken spin chains in $PbNi_2V_2O_8$ is $S = 1/2$. The data presented in Fig. 1 also imply that an increase in the defect concentration leads to a sizable increase in linewidth: the linewidth for a defect concentration of 0.02 per nickel ion is 0.5 T larger than for a 0.01 defect concentration. Such a significant increase in linewidth cannot be related to long-range dipole – dipole interaction (the respective local fields amount to about 0.01 T). Bearing in mind the multispin nature of magnetic defects, we can assume that the line broadening is related to contact between clusters. The magnitude of the broadening may be used to estimate the cluster's size. Assuming that this size is equal to the spin – spin correlation length ξ, we find that clusters come into contact in chain fragments whose length is on the order of 2ξ. The relative number of such chains is approximately $2x\xi$, where x is the impurity concentration, and ξ is measured in interspin distances. Thus, we find that for $x = 0.02$ the edges of a considerable fraction of clusters are in contact at $\xi \approx 10$.

Note that the exchange interaction of the Heisenberg type does not in itself lead to line broadening, but the presence of single-ion anisotropy (constant D) leads to what is known as anisotropic exchange interaction, which broadens the magnetic resonance lines.

3. Phase separation at the point of impurity-induced ordering

In a phase transition to an antiferromagnetic state, the magnetic resonance signal is usually transformed from the paramagnetic resonance signal to an antiferromagnetic resonance signal. The EPR frequency is determined by the properties of isolated magnetic ions, while the antiferromagnetic resonance frequency is determined by the oscillations of the order parameter. Thus, the phase transition to an ordered state is accompanied by a transformation of the magnetic resonance spectrum, and observation of this transformation makes it possible to determine the transition temperature and other characteristics of the phase transition. Previous studies of magnetic resonance in impurity-induced antiferromagnetic ordering of the spin system of a spin-Peierls magnet dealt with samples with high concentrations of impurities (more than 3%). In these samples the clusters are close to each other (separated by distances of the order of the correlation length ξ). For such concentrations, the transition to the antiferromagnetic state proved to be similar to a phase transition of ordinary 3D antiferromagnets. Let us compare the magnetic resonance spectra recorded in the vicinity of the phase transition point for various concentrations of impurities. Of special interest here is the case of low concentrations, when the distance between impurity atoms in chains exceeds ξ and the spin clusters are separated by remnants of the singlet matrix.

Figure 3 shows the evolution of the magnetic resonance spectrum in transition through the Néel point for a doped spin-Peierls magnet $Cu_{1-x}Mg_xGeO_3$ with $x = 0.017$. Clearly, as the temperature becomes lower, the paramagnetic resonance line splits into two lines. One corresponds to paramagnetic resonance: the values of the resonance field are temperature-independent and coincide with that of the resonance field for the paramagnetic phase. The position of the second line is temperature-dependent, and the frequency-vs.-field dependence for this line (see Ref. [18]) corresponds to the antiferromagnetic resonance spectrum for a biaxial antiferromagnet. There is a temperature range in which both lines (both antiferromagnetic and paramagnetic resonance) can be observed simultaneously. The temperature dependence of the intensities of the two spectral components is shown in Fig. 4. The possibility that the two magnetic resonance lines coexist because of the macroscopic inhomogeneity of the sample can be excluded because of the careful monitoring of the homogeneity in the impurity distribution over the sample and the small temperature interval of the transition (0.1 K). It is impossible to use the single-phase picture to explain the presence of two resonance modes in the sample: the antiferromagnetic phase is associated with order-parameter oscillations, which automatically excludes a paramagnetic resonance mode. Moreover, the paramagnetic phase does not allow for line splitting. A possible explanation of the coexistence of two resonance modes is the microscopic phase separation of the sample into paramagnetic and

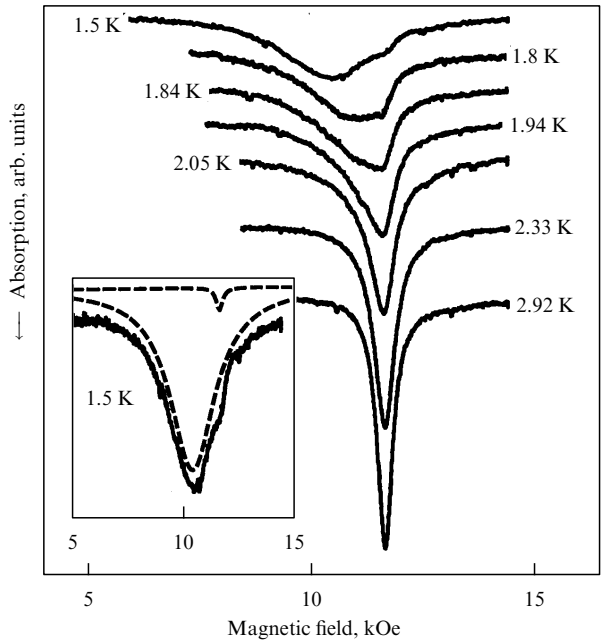

Figure 3. Evolution of the electron paramagnetic resonance spectrum for a $Cu_{0.983}Mg_{0.017}GeO_3$ sample in transition through the Néel point ($T_N = 2.25$ K). The measurements were done at 36 GHz with $\mathbf{H} \parallel \mathbf{b}$. The inset shows the resonance line at $T = 1.5$ K and its representation in the form of two Lorentzian lines.

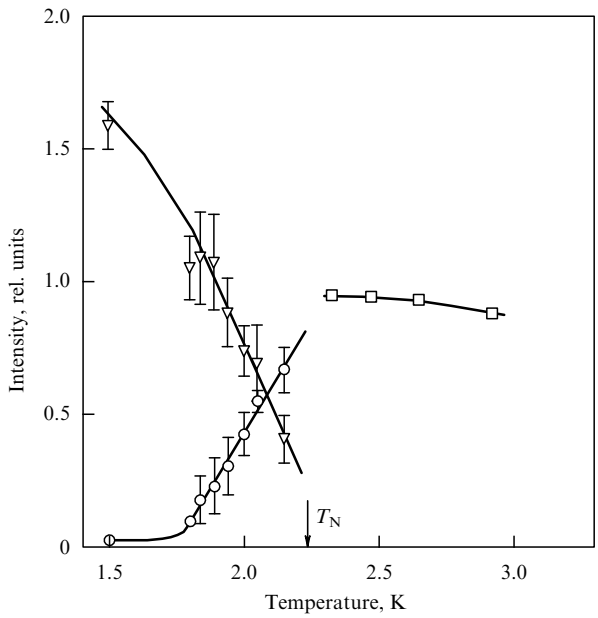

Figure 4. Temperature dependence of the intensities of the paramagnetic (circles) and antiferromagnetic (triangles) components of the magnetic resonance spectra for a $Cu_{0.983}Mg_{0.017}GeO_3$ sample. The squares indicate the temperature dependence of the intensity of the EPR signal in the paramagnetic phase.

antiferromagnetic regions. Indeed, let us examine spin clusters that arise around impurity atoms and assume that a coherent local antiferromagnetic order exists in a region of size L that meets the condition

$$k_B T = JS^2 \exp\left(-\frac{2L}{\xi}\right). \quad (1)$$

Here, J is the exchange integral along the chains. At distances greater than L, the antiferromagnetic correlations are destroyed by thermal fluctuations. We also assume that in transverse directions the antiferromagnetic correlations propagate over distances proportional to the exchange integrals in the corresponding directions. In this way, we arrive at a simple model (Fig. 5) in which elliptically shaped antiferromagnetic regions exist near each impurity center. The length of the ellipse along the chains is given by Eqn (1), while in the transverse directions it is smaller, in accordance with the exchange-integral ratios. At high temperatures (Fig. 5a), the regions of local antiferromagnetic order are not in contact, the order parameters for these regions do not correlate, and long-range antiferromagnetic order is absent, while each cluster contributes to the susceptibility of the sample and to the magnetic resonance signal in accordance with the fact that the cluster has a finite total magnetic moment. Hence, both the susceptibility and the magnetic resonance spectrum are of a paramagnetic nature. As the temperature is lowered, the clusters grow in size and some of them come into contact (Fig. 5b), which leads to the

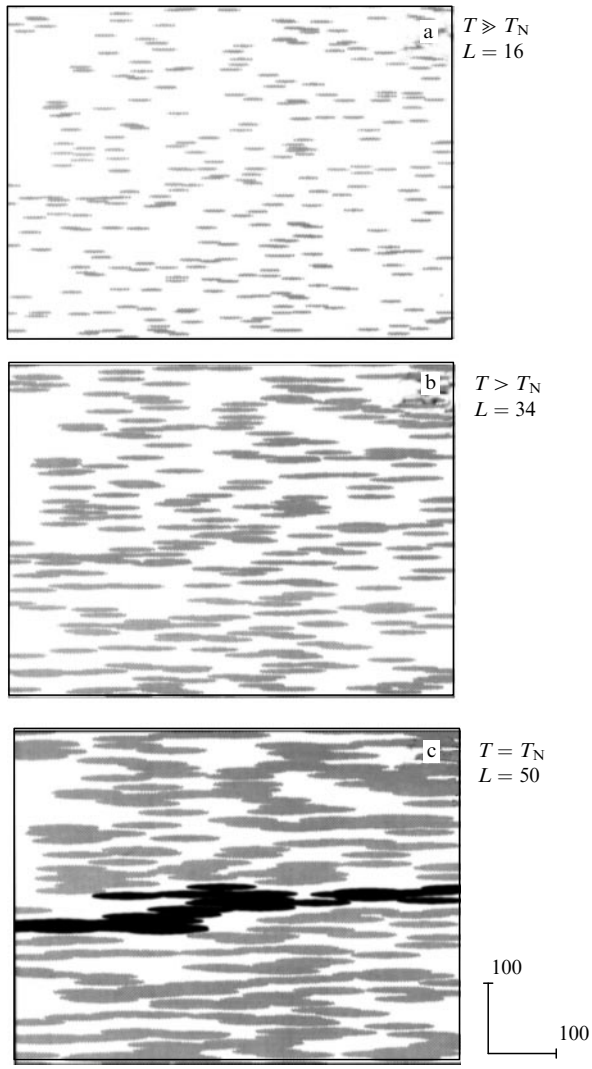

Figure 5. Simplified two-dimensional model of an impurity-induced phase transition. Gray areas are regions of local antiferromagnetic order, white areas mark remnants of the singlet matrix, and the black area represents a region of local antiferromagnetic order of the largest size.

formation of much larger regions with coherent antiferromagnetic order, regions that encompass several impurity atoms. Finally, Fig. 5c shows that there emerges a region of antiferromagnetic order, which penetrates the entire sample. The emergence of such a region corresponds to the percolation threshold in the problem of percolation of interpenetrating spheres [19]. Both at and near this value of L, the sample still has (Fig. 5c) single clusters that have finite magnetic moments and are isolated from the large antiferromagnetic regions by remnants of the singlet matrix. The free spins of these clusters continue to generate paramagnetic resonance signals, just as they do above the transition point. Note that percolation occurs not along impurity atoms but along regions of local antiferromagnetic order surrounding the impurity atoms. Thus, near the Néel point there are three types of regions: (1) very large regions of local antiferromagnetic order that generate antiferromagnetic resonance signals; (2) regions of the singlet matrix, which produce no magnetic response; and (3) single clusters, which are separated from the antiferromagnetic region by remnants of the singlet matrix and generate a paramagnetic signal.

We discovered a similar coexistence of signals of antiferromagnetic resonance and paramagnetic resonance in our studies of the impurity-induced antiferromagnetic ordering in the Haldane magnet $PbNi_2V_2O_8$ [20].

The picture of microscopic phase separation agrees with the results of 2D computer simulations performed by the Monte Carlo method for the ground states of spin-Peierls and Haldane systems with impurities [8]. The authors of this paper allowed for weak interchain interactions and found that near spin vacancies there are antiferromagnetically correlated finite spin projections (peaks in the local order parameter), while the space between the peaks is filled with a slightly perturbed singlet matrix. An important result achieved by this computer model was the demonstration that the order parameter is strongly modulated (about 100%). Assuming that at finite temperatures the vanishingly small order parameter in the regions between the impurities is destroyed by thermal fluctuations, we arrive at the conclusion that, topologically, the structure obtained through computer simulation and the percolation model we have just described are equivalent.

We are grateful to L N Dem'yanets and A Ya Shapiro for preparing the $PbNi_2V_2O_8$ samples and to T Masuda and K Uchinokura for supplying the $Cu_{1-x}Mg_xGeO_3$ samples and for the discussions concerning our results. The work was supported by a grant from the Russian Foundation for Basic Research (Project No. 00-02-17317).

References

1. Haldane F D M *Phys. Rev. Lett.* **50** 1153 (1983)
2. des Cloizeaux J, Pearson J J *Phys. Rev.* **128** 2131 (1962)
3. Bulaevskiĭ L N *Fiz. Tverd. Tela* **11** 1132 (1969) [*Sov. Phys. Solid State* **11** 921 (1969)]
4. Pytte E *Phys. Rev. B* **10** 4637 (1974)
5. Shender E F, Kivelson S A *Phys. Rev. Lett.* **66** 2384 (1991)
6. Fukuyama H, Tanimoto T, Saito M *J. Phys. Soc. Jpn* **65** 1182 (1996)
7. Khomskii D, Geertsma W, Mostovoy M *Czech. J. Phys. Suppl.* **46** (S6) 3239 (1996)
8. Yasuda C et al. *Phys. Rev. B* **64** 092405 (2001)
9. Glazkov V N et al. *J. Phys.: Condens. Matter* **10** 7879 (1998)
10. Smirnov A I *Usp. Fiz. Nauk* **170** 692 (2000) [*Phys. Usp.* **43** 642 (2000)]
11. Regnault L P et al. *Europhys. Lett.* **32** 579 (1995)
12. Masuda T et al. *Phys. Rev. Lett.* **80** 4566 (1998)
13. Uchiyama Y et al. *Phys. Rev. Lett.* **83** 632 (1999)
14. Hagiwara M et al. *Phys. Rev. Lett.* **65** 3181 (1990)
15. Miyashita S, Yamamoto S *Phys. Rev. B* **48** 913 (1993)
16. Katsumata K *J. Phys.: Condens. Matter* **12** R589 (2000)
17. Al'tshuler S A, Kozyrev B M *Elektronnyĭ Paramagnitnyĭ Rezonans Soedineniĭ Elementov Promezhutochnykh Grupp* (Electron Paramagnetic Resonance in Compounds of Transition Elements) 2nd ed. (Moscow: Nauka, 1972) [Translated into English (New York: Wiley, 1974)]
18. Glazkov V N et al. *Phys. Rev. B* **65** 144427 (2002); cond-mat/0105246
19. Shante V K S, Kirkpatrick S *Adv. Phys.* **20** 325 (1971)
20. Smirnov A I et al. *Phys. Rev. B* **65** 174422 (2002)